

Finite Element Simulation and Experiment of Chip Formation Process during High Speed Machining of AISI 1045 Hardened Steel

C.Z.Duan^{1,2}, T.Dou¹, Y.J.Cai², Y.Y.Li¹

¹Dalian University of Technology/School of Mechanical Engineering/Institute of Die and Mould, Dalian, China

Email: dcz71@163.com

²Tianjin University of Technology and Education/Tianjin Key Laboratory of High Speed Cutting & Precision Machining, Tianjin, China

Abstract—As an advanced manufacturing technology which has been developed rapidly in recent years, high speed machining is widely applied in many industries. The chip formation during high speed machining is a complicated material deformation and removing process. In research area of high speed machining, the prediction of chip morphology is a hot and difficult topic. A finite element method based on the software ABAQUS which involves Johnson-Cook material model and fracture criterion was used to simulate the serrated chip morphology and cutting force during high speed machining of AISI 1045 hardened steel. The serrated chip morphology and cutting force were observed and measured by high speed machining experiment of AISI 1045 hardened steel. The effects of rake angle on cutting force, sawtooth degree and space between sawteeth were discussed. The investigation indicates that the simulation results are consistent with the experiments and this finite element simulation method presented can be used to predict the chip morphology and cutting force accurately during high speed machining of hardened steel.

Index Terms—finite element simulation, high speed machining, serrated chip, chip formation, hardened steel

I. INTRODUCTION

As an advanced manufacturing technology which has been developed rapidly in more than last ten years, high speed machining can provide high efficiency of production and low cost, as well as improve the quality of machined surface. In addition, it can remove the difficult-to-cut materials with high hardness. High speed machining technology is widely applied in many industrial fields such as aeronautics and astronautics, automobile, mould, light industry, etc. One of the most important differences on cutting mechanics between high speed machining and conventional machining is that in high speed machining, a serrated chip is most often generated which affects nearly every aspect of high speed machining process, such as cutting force[1], cutting temperature[2], cutting tool wear[3] and life and machined surface quality[4]. Therefore, it is necessary to investigate and to predict the formation of serrated chip and the effect of chip morphology on vibration of cutting force, and their relationship with workpiece material and machining condition. At present, the published researches on prediction of serrated chip formation have focused on the theoretical modeling and the finite element simulation[5-6]. High speed machining is a strongly non-linear and complex contact

process. But these characteristics, especially the material constitutive relationship in high deformation condition are not fully considered by the existing methods. In addition, the simulation results of commonly used Deform-2D FE software are usually not consistent with the experiments because of their weak capability for non-linear problems. In this paper, a finite element method involving Johnson-Cook material model and fracture criterion was used to simulate the serrated chip formation during high speed machining using commercial FE software ABAQUS which can in principle handle such strongly non-linear problems and allow the definition of complex contact conditions. By using above method for FE simulation, the chip morphology during high speed machining of AISI 1045 hardened steel was accurately predicted and the effects of rake angle on the chip morphology and cutting force were discussed.

II. CHIP MORPHOLOGY SIMULATION

A. Material Model

For the simulation of chip morphology and cutting force, a Johnson-Cook model was used. This model is a strain rate and temperature dependent[7-8] visco-plastic material model which describes the relationship of stress, strain, strain rate and temperature. It is suitable for problems where the strain rate varies over a large range (10^2s^{-1} to 10^6s^{-1}), and the temperature changes due to plastic deformation caused by thermal softening. This model uses the following equivalent flow stress:

$$\bar{\sigma} = [A + B(\bar{\epsilon})^n] \left[1 + C \ln \left(\frac{\dot{\bar{\epsilon}}}{\dot{\bar{\epsilon}}_0} \right) \right] \left[1 - \left(\frac{T - T_0}{T_{melt} - T_0} \right)^m \right] \quad (1)$$

Where $\bar{\sigma}$ is the equivalent stress, $\bar{\epsilon}$ is the equivalent plastic strain, $\dot{\bar{\epsilon}}$ is the plastic strain rate, $\dot{\bar{\epsilon}}_0$ is the reference strain rate (1.0s^{-1}), T_0 is the room temperature, T_{melt} is the melting temperature, A is the initial yield stress (MPa), B is the hardening modulus, n is the work-hardening exponent, C is a coefficient dependent on the strain rate (MPa), and m is the thermal softening coefficient. The Johnson-Cook parameter values used to simulate the behaviour of AISI 1045 workpiece are specified in Table I.

TABLE I
JOHNSON-COOK BEHAVIOUR LAW PARAMETERS OF AISI-1045

A (MPa)	B (MPa)	n	C	m	$\dot{\epsilon}_0 (s^{-1})$	$T_{mel} (\delta)$	$T_0 (\delta)$
553	600	0.234	0.0134	1.0	0.001	1460	20

The material constants for Johnson-Cook model are identified through high strain rate deformation tests using split Hopkinson's bar. Moreover, the material deformation in primary shear zone during high speed machining is a typical deformation process at high strain rate. Therefore, Johnson-Cook model is used to simulate the chip morphology and cutting force during high speed machining.

B. Chip Fracture Criterion

In order to simulate the separation between chip and workpiece, a dynamic failure model was used for the Johnson-Cook model in ABAQUS/Explicit which is suitable only for high strain-rate deformation of metals. The Johnson-Cook dynamic failure model is based on the value of the equivalent plastic strain at element integration points. The failure is assumed to occur when the damage parameter D exceeds 1. This is a physical criterion. The damage parameter D is defined as follows:

$$D = \sum \left(\frac{\Delta \bar{\epsilon}^{pl}}{\bar{\epsilon}_f^{pl}} \right) \quad (2)$$

where $\Delta \bar{\epsilon}^{pl}$ is the increment of equivalent plastic strain, $\bar{\epsilon}_f^{pl}$ is the strain at failure, and the summation is performed over all increments in the analysis. The strain at failure $\bar{\epsilon}_f^{pl}$ is assumed to be dependent on the nondimensional plastic strain rate $\dot{\bar{\epsilon}}^{pl} / \dot{\epsilon}_0$, the dimensionless pressure-deviatoric stress ratio p/q (where p is the pressure stress and q is the Mises stress), and the non-dimensional temperature $\hat{\theta} = (T - T_0) / (T_{mel} - T_0)$ which is defined earlier in the Johnson-Cook hardening model. The dependence of $\bar{\epsilon}_f^{pl}$ is assumed to be separable and is the following relation[7]:

$$\bar{\epsilon}_f^{pl} = \left[d_1 + d_2 \exp \left(d_3 \frac{p}{q} \right) \right] \left[1 + d_4 \ln \left(\frac{\dot{\bar{\epsilon}}^{pl}}{\dot{\epsilon}_0} \right) \right] \left(1 + d_5 \frac{T - T_0}{T_{mel} - T_0} \right) \quad (3)$$

where $d_1 - d_5$ are failure parameters measured at or below the transition temperature T , and $\dot{\epsilon}_0$ is the reference strain rate. The values of $d_1 - d_5$ are specified in Table II when the Johnson-Cook dynamic failure model was defined.

 TABLE II
JOHNSON-COOK DAMAGE LAW PARAMETERS OF AISI -1045

Damage law parameters	AISI 1045 steel
d1	0.06
d2	3.31
d3	-1.96
d4	0.0018
d5	0.58

C. Friction Model

In this paper, the finite element simulation is found based on the friction modeling of Coulomb Law.

$$\begin{cases} \tau_f = \mu \sigma_n & \mu \sigma_n < \bar{\tau}_s \quad (\text{flow area}) \\ \tau_f = \bar{\tau}_s & \mu \sigma_n \geq \bar{\tau}_s \quad (\text{cohesive area}) \end{cases} \quad (4)$$

Where τ_f is the friction stress, μ is the friction coefficient,

σ_n is the normal stress, $\bar{\tau}_s$ is the limited shear stress of the material.

Here, a surface contact model in ABAQUS/Explicit was used to simulate the contact between chip and tool. The friction coefficients of cohesive and flow area are 1 and 0.27 respectively[9]. The ABAQUS can estimate the contact type based on the actual contact stress and select proper friction model.

D. Finite Element Modeling of High Speed Machining

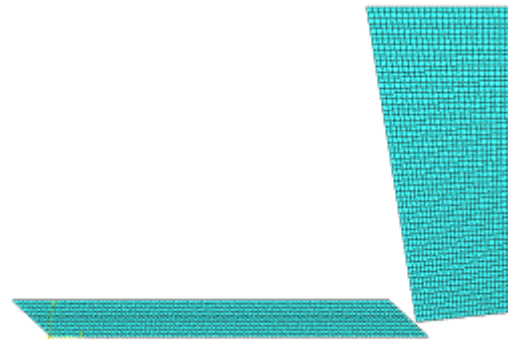


Figure 1. 2D finite element model building of orthogonal cutting

The workpiece was discretized using 4-node bilinear elements with reduced integration (CPE4R). In order to obtain a better astringency at the original stage of finite element simulation, the mesh was oriented at a specified angle to the cutting plane. The 2D orthogonal cutting modeling is shown in Fig.1. The mesh division of the workpiece into 80×12 elements was performed. The mesh division of the tool into 58×25 was performed when the rake angle is -10°. The simulation and following experiment were carried out in the same cutting conditions.

III. EXPERIMENT OF HIGH SPEED MACHINING

A. Experimental Material

AISI 1045 steel was selected as the experiment material. The hardness HRC45 required was obtained by quenching

with 850 in 70 minutes and tempering with 430 in 5 hours. The high speed machining experiment was carried out on CA6140 lathe using insert carbide tool (YT15) under dry cutting condition. The cutting forces were measured by a YDX-9702 turning dynamometer, as seen in Fig. 2. The assembly is shown in Fig. 3.

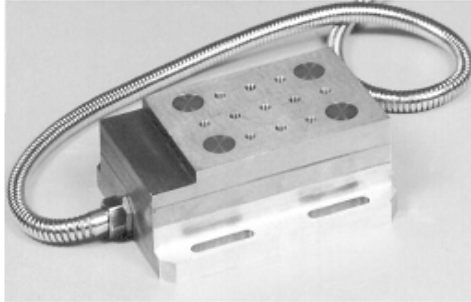


Figure 2. Workpiece, cutting tool and dynamometer installation

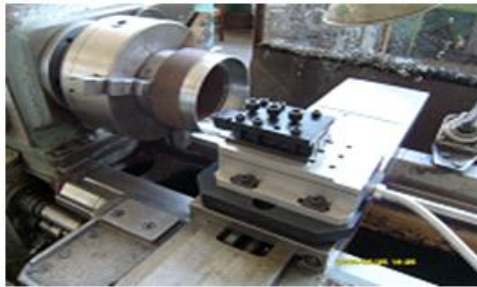


Figure 3. Workpiece, cutting tool and dynamometer installation

B. Experiment Process

In order to get higher linear cutting speed, the workpieces with larger diameter were adopted. The steel ingots were machined into cylinders with diameter 153mm and thickness 2.5mm, as shown in Fig. 3. Then heat treatment was used to get proper hardness. The orthogonal high speed cutting was carried out in lathe under dry cutting condition. The tool was replaced in time to make sure that the tool tip remains sharp enough. Different tool angles were adopted. The cutting parameters are as follows: cutting thickness is 0.2mm, cutting width is 2.5mm, cutting speed is 433m/min, tool rake angles are -10° , 0° and 10° respectively. The chips formed with different cutting parameters were set vertically into the mixture of epoxy resin and curing agent. After sanding, polishing and eroding, chip morphology and microstructure were observed and measured by using a Neuphot- optical microscope. The metallographic specimen is shown in Fig. 4.

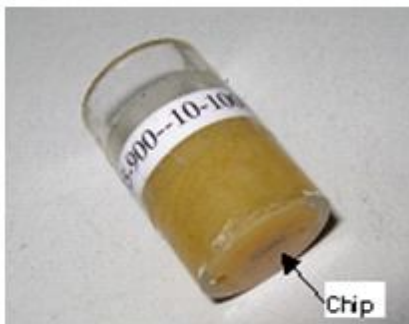


Figure 4. Metallurgical sample

II COMPARISON BETWEEN SIMULATION AND EXPERIMENT

The comparisons between the predicted serrated chip morphology of FE simulation and the experimental results with three different rake angles are shown in Fig. 5, Fig. 6 and Fig. 7 respectively.

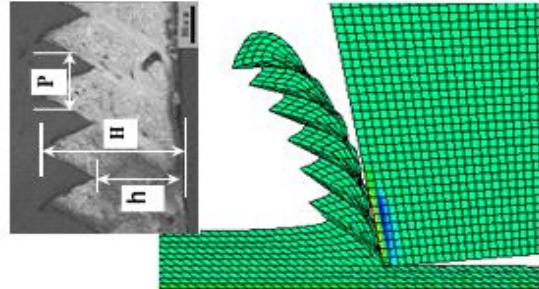


Figure 5. Comparison between experimental and modeling serrate chip morphology when tool rake angle is -10°

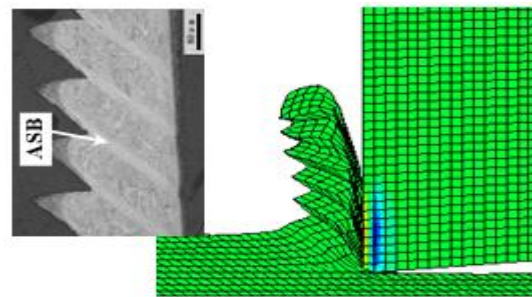


Figure 6. Comparison between experimental and modeling serrate chip morphology when tool rake angle is 0°

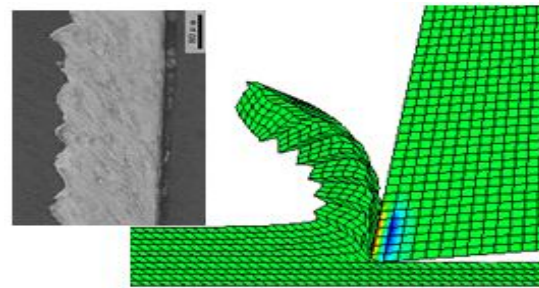


Figure 7. Comparison between experimental and modeling serrate chip morphology when tool rake angle is 10°

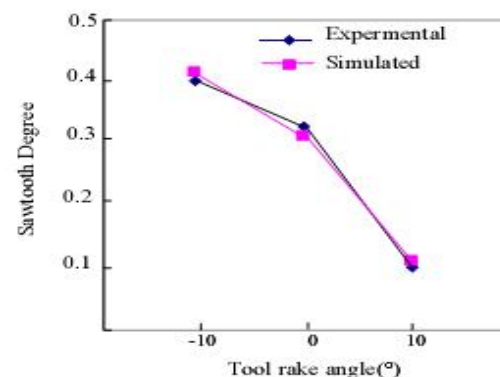


Figure 8. Comparison between experimental and simulated sawtooth degree under different tool rake angles

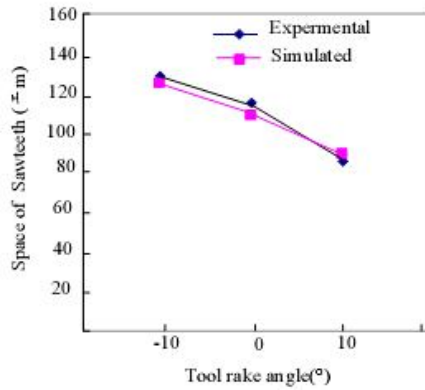


Figure 9. Comparison between experimental and simulated space of sawteeth under different tool rake angles

As seen in these figures, the effect of rake angle on chip morphology is significant, specially, serrated chip is formed easily when use a negative rake angle. Generally, the sawtooth degree G_s and the space between sawteeth P can describe the morphology and deformation of serrated chip qualitatively[9,10]. is defined as follows:

$$G_s = (H - h) / H \quad (5)$$

G_s and P can be measured in the method shown in Fig.5, and their relationship with the tool rake angles are shown in Fig.8 and Fig.9 respectively. The comparisons show that simulation results are well consistent with the experiments and the sawtooth degree decreases with increasing tool rake angle when the cutting speed and feed are fixed. During the experimental process, the clear adiabatic shear bands were found inside the serrated chips (see Fig.6), which indicates that the main reason to generate serrated chip is the occurrence of adiabatic shear instability in the primary shear zone. As shown in Fig.10, Fig.11 and Fig.12, the tool rake angle has a main influence on the cutting force and the values of main cutting force decreases with increasing tool rake angle. It also can be seen that the cutting forces start to increase since the tool acts on the workpiece and get in a regular vibration when the cutting process is steady. It is noted that the vibration frequency of cutting forces is consistent with that of sawtooth formation and the vibration amplitude of the main cutting force increases with the increase of sawtooth degree. These phenomena indicate that the serrated chip formation results in a regular vibration of cutting forces.

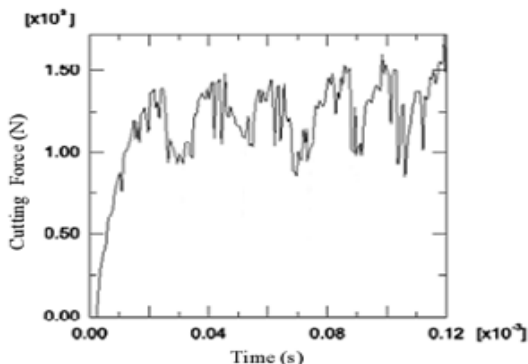


Figure 10 Curve of main cutting force when tool rake angle is -10° during simulation

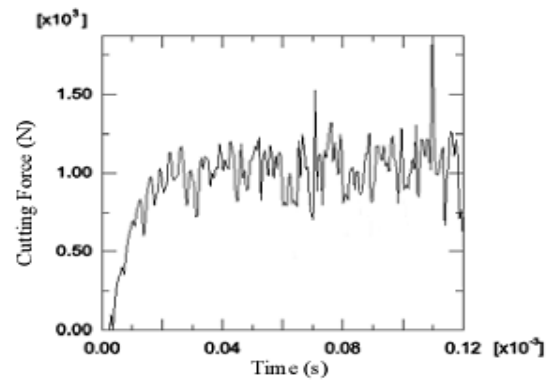


Figure 11. Curve of main cutting force when tool rake angle is 0° during simulation

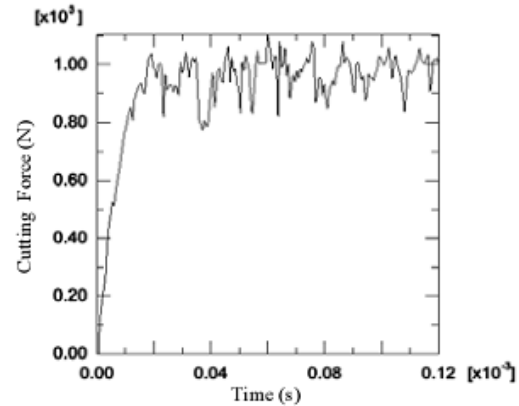


Figure 12 Curve of main cutting force when tool rake angle is 10° during simulation

Fig.13 is the comparison of average cutting forces between the simulation and experiments. The contrast curves show that the simulation results are well consistent with the experiments and the average cutting forces decrease with increasing the rake angle, which further indicate that the methods for FE simulation presented in this paper is feasible. According to the FE simulation, the cutting process can be optimized by choosing proper parameters.

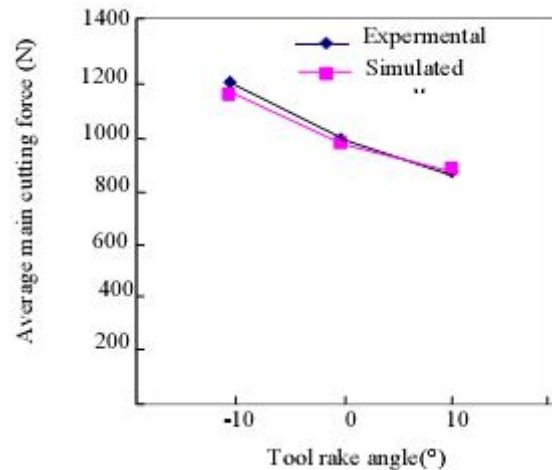


Figure 13. Comparison between experimental and simulated average main cutting force under different tool rake angles

CONCLUSIONS

The aim of the present work is to simulate the chip morphology and cutting forces during high speed machining of AISI 1045 hardened steel by using Johnson-Cook material model based on commercial FE software ABAQUS. A physical fracture criterion suited to high deformation condition and a dynamic failure model in ABAQUS/Explicit to carry out the separation between chip and workpiece were utilized. The effects of rake angle on the chip morphology and cutting force were discussed and testified by high speed machining experiments. The investigation indicates that the simulation results are well consistent with the experiments. The serrated chip comes out during high speed machining of AISI 1045 hardened steel. The sawtooth degree, cutting forces and the space between sawteeth increase with decreasing tool rake angle when the other cutting conditions are fixed. Therefore, the FE simulation method presented in this paper can be used to predict the chip formation and cutting force accurately during high speed machining of hardened steel.

ACKNOWLEDGMENT

This research is sponsored by the China Natural Science Foundation(No.50875033) and by the Natural Science Key Foundation of Tianjin (No.08JCZDJC18400)and by Tianjin Key Laboratory of High Speed Cutting & Precision Machining.

REFERENCES

- [1] G. Sutter, A. Molinari, "Analysis of the cutting force components and friction in high speed machining," *J. Manuf. Sci. Eng.* vol.127, pp. 245-250, 2005.
- [2] G. Sutter, N. Ranc, "Temperature fields in a chip during high-speed orthogonal cutting-An experimental investigation," *Inter. J. Machine Tools Manuf.* vol.47, pp.1507-1517, 2007.
- [3] Z.N. Farhat, "Wear mechanism of CBN cutting tool during high-speed machining of mold steel," *Mater. Sci. Eng.* vol.A361, pp.100-110, 2003.
- [4] T.I. El-Wardany, H.A. Kishawy, and M.A. Elbestawi, " Surface integrity of die material in high speed hard machining, Part I: micrographical analysis," *J. Manuf. Sci. Eng.* vol. 122, pp.620-631, 2000.
- [5] Sung-Han Rhim, Soo-Ik Oh, "Prediction of serrated chip formation in metal cutting process with new flow stress model for AISI 1045 steel," *J. Mater. Process. Technol.* vol.171, pp.417-422, 2006.
- [6] T.J.Burns, M.A.Davies, "On repeated adiabatic shear band formation during high-speed machining," *Inter. J. Plasticity*, vol.18, pp.487-506, 2002.
- [7] T.Mabrouki, J.-F.Rigal, "A contribution to a qualitative understanding of thermo-mechanical effects during chip formation in hard turning," *J. Mater. Process. Technol.* vol.176, pp.214-221, 2006.
- [8] F.Klocke, H.-W.Raedt, and S.Hoppe, "2D-FEM simulation of the orthogonal high speed cutting process," *Machining Science and Technology*, vol. 5 (3), pp.323-340, 2001.
- [9] M.A.Davies, A.L.Cooke, and E.R.Larsen, "High Bandwidth Thermal Microscopy of machining AISI 1045 Steel," *CIRP Annals-Manufacturing Technology*, vol. 54 (1), pp.63-66, 2005.
- [10] M.A.Davies, Q.Cao, and A.L.Cooks et al, "On the measurement and prediction of temperature fields in machining AISI 1045 Steel," *CIRP Annals-Manufacturing Technology*, vol. 52 (1), pp. 77-80, 2003.